Computational Modeling of Patellofemoral Joint Motion of Human Knee

Jeffry Hartanto
Dept. of Computer Science, National University of Singapore
Emails: jhartanto@comp.nus.edu.sg

Abstract

Knee joint is the largest joint in the human body. Inspite of its important roles, it has a fairly unstable joint design and can degenerate over time. For most of the knee joint problems, surgical intervention is needed to restore normal knee joint functionality. However, knee surgery is a complex operation. If the surgery is not performed correctly, it may introduce pain on the knee, abnormal knee motion and accelerate the degenerative process of the knee. Therefore, precise pre-operative planning is very important to ensure normal knee functionality after the surgery. One approach to pre-operative planning is to model knee joint function computationally. Due to the complexity of the interactions, modeling of knee joint function is a challenging task. Existing models of knee joint function are appropriate only for medical research but not routine clinical practice for pre-operative surgery planning. Our overall research aims to resolve this issue by developing a subject-specific knee model that is appropriate for routine clinical practice. As a start, this QE paper focuses on modeling the patellofemoral joint, which is the simplest joint that makes up the whole knee joint.

1 Introduction

Knee joint is the largest joint in the human body [1] (Fig. 1). This joint supports the whole body weight and allows a complex set of movements such as walking, jumping and running. Inspite of its important roles, the knee joint has a fairly unstable joint design and can degenerate over time. Knee joint injuries such as torn ligaments, torn tendons, torn meniscus, cartilage lesion, patellar dislocation and osteoarthritis are common problems among people of all ages, especially athletes. In particular, osteoarthritis occurs more in the knee than any other joint [2]. For most of the knee joint problems, surgical intervention is needed to restore normal knee joint functionality.

Knee surgery is a complex operation. For example, in medial patellofemoral ligament (MPFL) reconstruction surgery, a slight change on insertion site of the ligament can affect the possible range of knee articulation. If the surgery is not performed correctly, it may introduce pain on the knee, abnormal knee motion and accelerate the degenerative process of the knee. Therefore, precise pre-operative planning is very important to ensure normal knee functionality after the surgery.

One approach to pre-operative planning is to model knee joint function computationally, and to use the model to predict possible surgical outcome. To achieve this goal, the model needs to correctly capture the 3D geometries of the patient's knee bones and simulate the interactions between bones and soft tissues. Due to the complexity of the interactions, modeling of knee joint function is a challenging task.

Existing models of knee joint function can be grouped into four categories: abstract models, static models, kinematic models and dynamic musculoskeletal models. Abstract models [3, 4] do not model the 3D geometries of bones and soft tissues. Thus, they cannot model the interactions between physical bones and soft tissues. Static models [5, 6, 7] model the poses of knee bones at prescribed flexion angles. Methods for static models directly construct 3D bone poses at prescribed flexion angles from CT or MRI images of a patient's knee. They are simple and accurate but cannot model the full range of knee motion.

Kinematic models [8, 9, 10, 11, 12, 13] model the poses of knee bones over a range of flexion angles without considering forces. Methods for kinematic models capture 3D geometries of knee bones at neutral pose from CT or MRI images. In addition, they use knee motion data obtained from low-resolution MRI sequence, fluoroscopic video or motion capture (mocap) system to determine knee bone poses over a range of flexion angles. Dynamic musculoskeletal models [14, 15, 16, 17, 18, 19, 20, 21, 22, 23, 24, 25, 26, 27] model the poses of knee bones and forces over a range of flexion angles. Methods for dynamic models apply the kinematic method with mocap data to obtain bone poses, and adopt various muscle models to model muscle forces. Due to the complexity of kinematic and dynamic models, they are used primarily in medical research and are not appropriate for routine clinical practice.

The overall objective of this research is to develop a novel model of knee joint function that is appropriate for routine clinical practice. The knee consists of two joints, namely the tibiofemoral (TF) joint and the patellofemoral (PF) joint. PF joint is simpler than TF joint. So, this QE paper first focuses on modeling PF joint motion. The model should be easy to construct and to apply in routine clinical practice.

2 Functional Anatomy of Human Knee Joint

The knee consists of four bones, namely, femur, tibia, fibula, and patella, and soft tissues, including cartilages, ligaments, muscles and tendons [28] (Fig. 1). Cartilages are located at the end of femur and tibia, and at the back of patella. They protect the bones by providing extremely slippery surfaces that allow two bones to slide on one another. Moreover, they also act as shock absorbers. Ligaments are tough tissues that are attached to two bones. They control the stability of the knee by constraining the range of motion of the bones. Muscles are attached to bones through tendons. They trigger bone motion by transferring the pulling forces generated from muscle

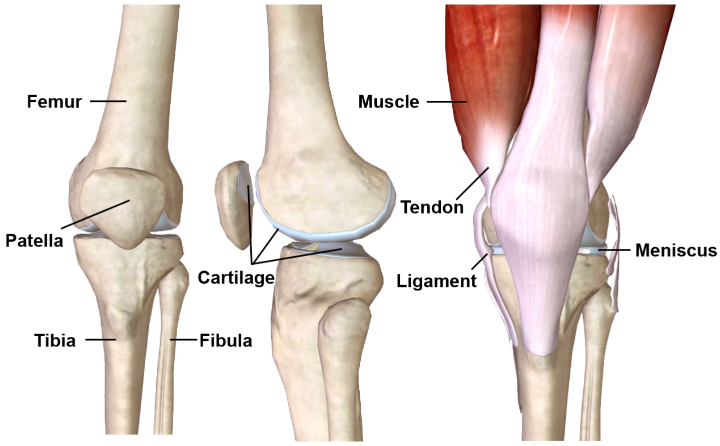

Figure 1: Anatomy of the left knee. The knee consists of bones and soft tissues [29].

(a)

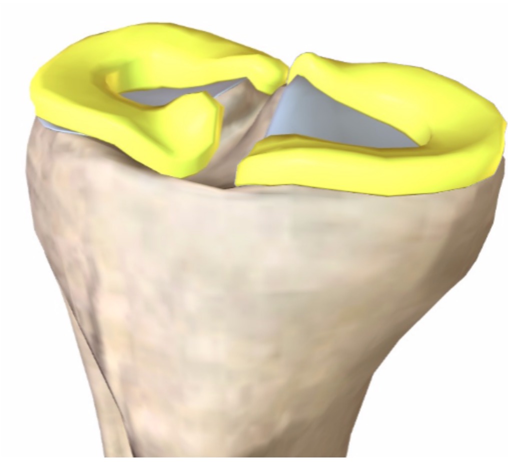

(b)

Figure 2: Protective soft tissues. (a) Cartilage (blue and dark gray), (b) menisci (yellow) [29].

contraction to bones through tendons.

The knee has two joints, namely, tibiofemoral (TF) and patellofemoral (PF) joints. Both joints consist of soft tissues such as cartilages, ligaments, muscles and tendons. Cartilages are thin layers of tissues whose shapes resemble those of the bone surfaces that they cover (Fig. 2a). TF joint has two menisci attached to the tibia that lie between the tibia and the femur. They are thick tissues with crescent shape that are concave on the top and flat at the bottom (Fig. 2b). They act as additional lubricating surfaces, shock absorbers and stabilizers of TF joint. In TF joint, the fibula is connected to the tibia by ligaments. However, it does not influence TF joint motion.

Knee motion consists of TF and PF joint motion. In general, each joint has six degrees of freedom of motion, three translations and three rotations, which can be described according to three axes, namely, x-, y- and z-axis (Fig. 3). The positive

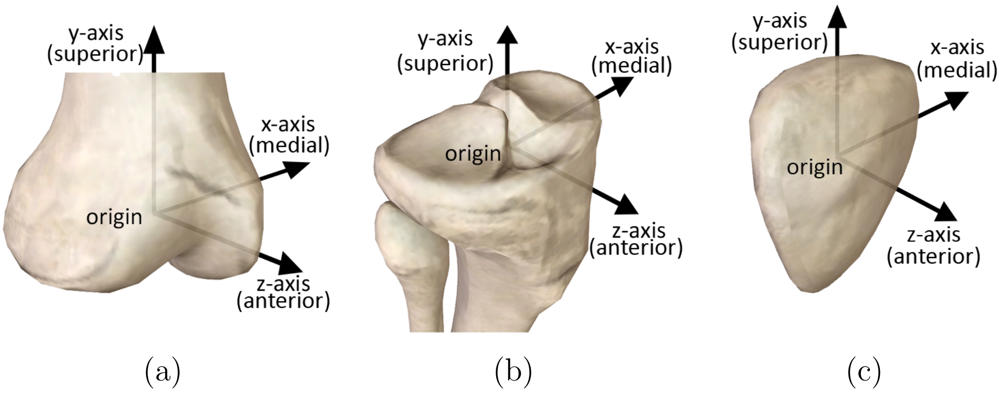

Figure 3: Origins and axes of right knee bones. (a) femur, (b) tibia, (c) patella [29].

x-axis points medially towards the middle of a subject's body, and the negative x-axis points laterally towards the side of a subject's body. The positive y-axis points superiorly towards a subject's head, and the negative y-axis points inferiorly towards a subject's foot. The positive z-axis points anteriorly towards the front of a subject's body, and the negative z-axis points posteriorly towards the back of a subject's body. The origin of the three axes are defined based on bony landmarks identifiable in medical images such as CT or x-ray images. Motion of a bone includes translation and rotation about its axes.

TF joint motion is the articulation between tibia and femur. It is triggered by muscle contraction which causes the tendons and the ligaments to become taut and pull on the tibia. Consider the TF joint at the neutral knee pose shown in Figure 4a. When the knee flexes, the pulling of the tibia causes the tibia, along with its cartilages and the menisci, to roll and slide posteriorly towards the back of the subject's body and superiorly upward (Fig. 4b). The flexion angle measures the angle between the femur and the tibia about the x-axis, and it ranges between $0°$ and $130°$ to $145°$. Conversely, when the knee extends, the tibia rolls and slides anteriorly towards the front of the subject's body. During knee flexion-extension, there is also a slight amount of rotation about the y-axis and z-axis, and translation about the x-axis [30].

PF joint motion is the articulation between patella and femur. The patella is constrained by ligaments and a tendon to rest on the femur. As the knee flexes, the patella, along with its cartilage, slide and roll posteriorly and inferiorly over the femur (Fig. 5a). Beyond flexion angle of about $30°$, the patella engages the groove of the femur (Fig. 5b) and locks in place. During knee flexion-extension, there is also a small amount of rotation about the y-axis and the z-axis, and translation about the x-axis. As the knee flexes, the patella contacts different parts of the femoral surface in turn (Fig. 6).

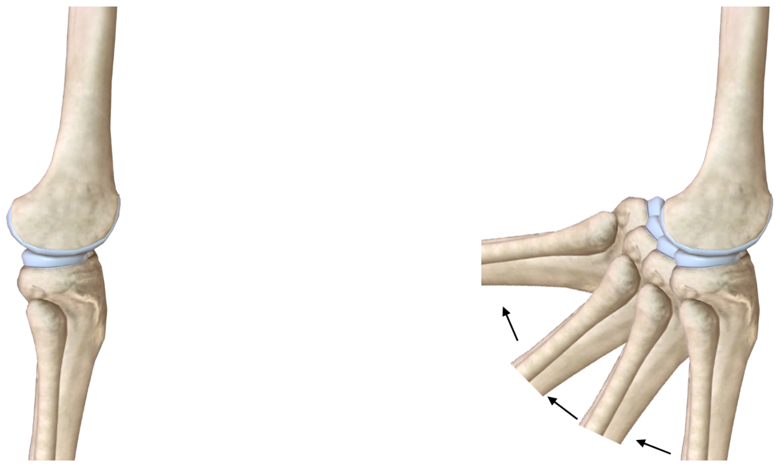

(a) (b)

Figure 4: Motion of TF joint. (a) Femur and tibia at neutral knee pose [29]. (b) Tibia rolls and slides with respect to femur when the knee flexes [29].

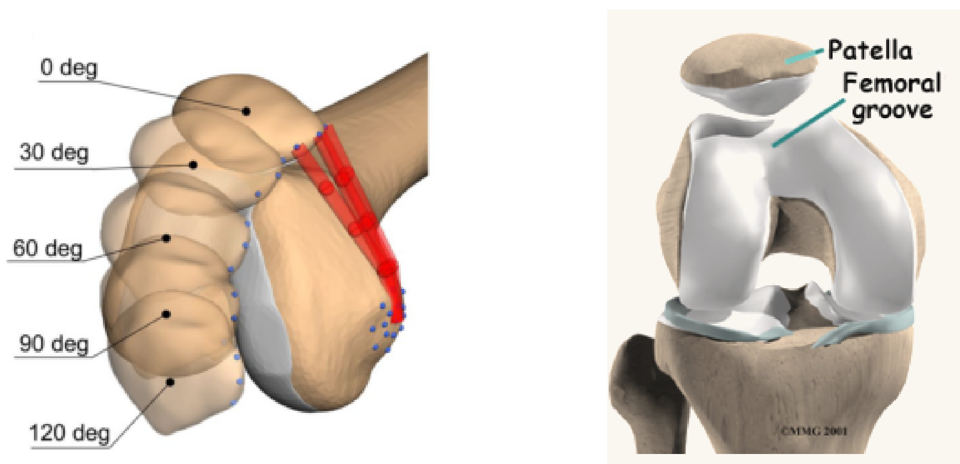

(a) (b)

Figure 5: Motion of PF joint. (a) Patella slides and rolls with respect to femur when the knee flexes [31]. (b) The patella engages the femoral groove after about 30° flexion angle [32].

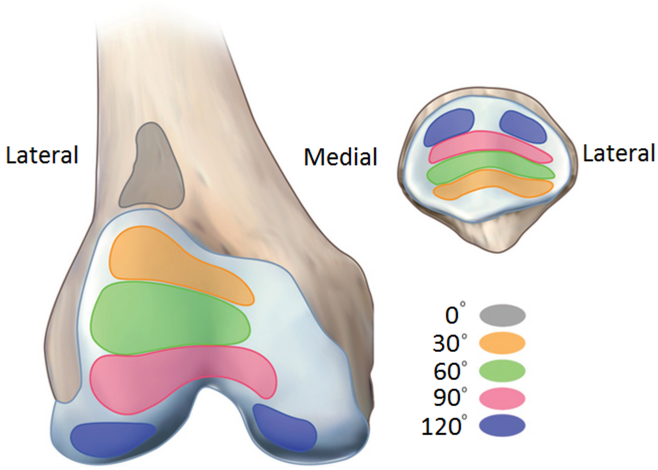

Figure 6: Illustration of patellofemoral contact area from 0° to 120° flexion angles of the right knee [33].

3 Existing Work

Existing work on knee joint modeling can be categorized according to the type of knee model adopted, namely, abstract models, static models, kinematic models and dynamic musculoskeletal models. Abstract models [3, 4], which are known as skeletal models in animation community, do not model the 3D geometries of bones and soft tissues in knee joint. Instead, they model a joint as two lines or more connected at a point (Fig. 7a). Thus, they cannot model the interactions between physical bones, ligaments and muscles. Therefore, they are omitted in the following discussion. On the other hand, static models, kinematic models and dynamic musculoskeletal models capture 3D geometries of the bones (Fig. 7b). Moreover, kinematic and dynamic models use both geometrical and abstract knee models (Fig. 7c).

3.1 Static Models

Static models [5, 6, 7] model the poses of knee bones at prescribed knee flexion angles without capturing joint motion. Methods that use static models apply computer-tomography (CT) or magnetic resonance imaging (MRI) to capture 3D images of a subject's knee at a small number of prescribed flexion angles, typically from 0° to 120° at intervals of 30°. Then, they segment CT or MRI images to construct 3D models of each knee bone at each flexion angle. In this way, they directly obtain the poses of the knee bones at prescribed flexion angles.

Static models can be used to model certain soft tissue properties. For example, [5, 6] measure the length of virtual MFPL given a knee pose. Since the MPFL is attached to the patella and the femur, its length varies for different knee poses. In this way, these methods can measure the length of MPFL at various knee poses and identify excessive length changes that can damage MPFL. On the other hand, [7] measures the length of posterior cruciate ligament (PCL) at various knee poses to

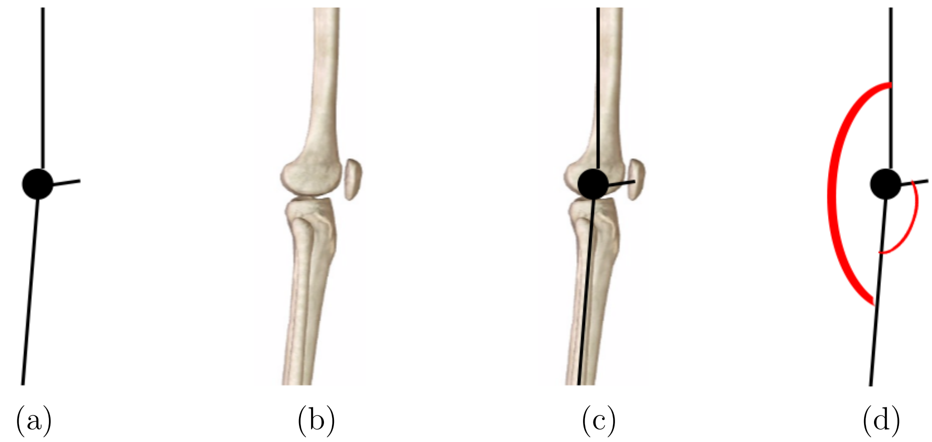

Figure 7: Types of knee model. (a) Abstract model, (b) geometrical model, (c) geometrical model aligned to abstract model, and (d) abstract model that includes bones (black) and muscles (red).

identify viable femoral attachment sites.

Static models have several benefits. They are subject specific and accurate because they directly construct a subject's 3D bone models from CT/MRI images. Moreover, they are very easy to apply because bones are very distinctive in CT/MRI images and can be easily segmented by image thresholding. Also, they do not require soft tissue modeling.

In principle, it is possible for static models to capture bone poses at very small flexion angle intervals and thus achieve knee motion modeling. However, this approach is not adopted in medical research and routine clinical practice because it requires a large amount of CT or MRI scans. Excessive CT scanning exposes a subject to an excessive amount of radiation, whereas excessive MRI scanning is very costly. Thus, static methods capture only a small number of bone poses, which are insufficient for modeling knee joint motion. Therefore, these models are called static models.

3.2 Kinematic Models

Kinematic models [8, 9, 10, 11, 12, 13] model the poses of knee bones over a range of flexion angles without considering forces. Methods that use kinematic models consist of two stages, namely **model calibration** and **knee motion generation**. In the model calibration stage, they first construct high-resolution 3D models of knee bones at a prescribed flexion angle, usually 0°. Next, they capture knee motion data through a range of flexion angles using low-resolution MRI [8, 9], fluoroscopic video [10, 11] or motion capture system [12, 13]. Then, they apply methods such as 3D-3D registration [8, 9], 3D-2D registration [10, 11] or inverse kinematic [12, 13] to obtain **model parameter values** and **joint kinematic data** of abstract bone model. The parameter values include the lengths of the abstract bones, and the joint kinematic data include a sequence of joint positions and angles over time.

In the motion generation stage (Fig. 8), they apply forward kinematics on the

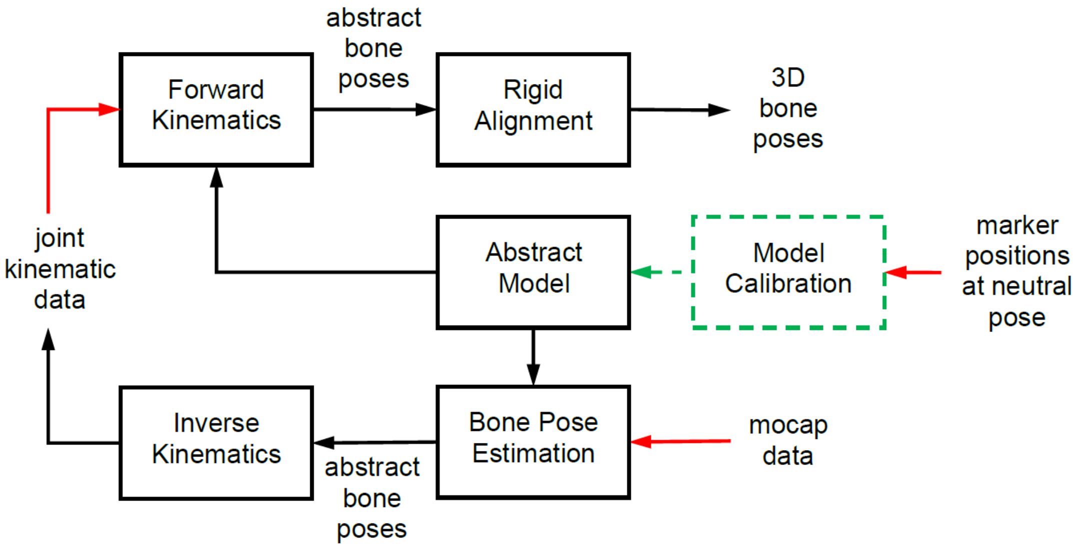

Figure 8: Kinematic method with mocap data. Inverse kinematics is used for model calibration, and forward kinematics is used for motion generation. Red arrows: inputs, black arrows: outputs, green: model calibration.

joint kinematic data, i.e., joint angles, to compute the poses of the abstract bones over time. Next, they align the 3D geometric bone models to the abstract bone poses to obtain 3D bone poses over time. In this way, they generate bone poses of abstract model over a range of flexion angles.

The various methods in this category primarily differ in the way they estimate abstract model parameter values and compute joint kinematics in the model calibration stage. The methods of [8] segment low-resolution MRI images and construct low-resolution bone models, whereas [9] construct low-resolution point cloud models. Then, they rigidly register each of the high-resolution 3D bone models to the low-resolution model using 3D-3D registration methods such as iterative closest point [34]. Finally, they align an abstract model to high-resolution 3D bone models to obtain abstract model parameter values and joint kinematic data.

The methods of [10, 11] segment 2D bone contours in each fluoroscopic video frame. Next, they perform 3D-2D registration by projecting 3D bone models to match the bone contours in the fluoroscopic video frame. 3D-2D registration is achieved by minimising registration error using general optimisation algorithms such as simulated annealing [10] and Powell's direction set method [11]. Next, they align an abstract model to high-resolution 3D bone models to obtain abstract model parameter values and joint kinematic data. To improve registration accuracy, the method of [11] captures three sets of MRI images at $0°$, $30°$ and $60°$, and use 3D bone models obtained from these MRI images to initialize the optimisation algorithm. Moreover, [11] also models stretchable patellar ligament which is attached to the patella and the tibia.

The methods of [12, 13] capture the motion of reflective markers attached to a subject's knee using motion capture (mocap) system (Fig. 8). First, they capture the marker positions of the knee at a neutral pose. Then, they use these marker positions to estimate the model parameters, i.e., bone lengths of the abstract model, as well as the relative positions of the markers with respect to the abstract bones. Next, they capture the marker positions of the knee as it flexes and extends. Then, they apply inverse kinematics on the mocap data and calibrated abstract model to compute the joint angles over time, which make up the joint kinematic data.

Kinematic models are subject specific because they construct a subject's 3D bone models from CT/MRI images. Moreover, they model bone poses over a range of flexion angles. Thus, they can model knee joint motion.

Kinematic models are more complex than static models because they require additional computations such as 3D-3D registration, 3D-2D registration or inverse kinematic. These additional computations incur additional errors on modeling accuracy. The method that uses motion capture system [12, 13] is prone to marker position errors when skin deforms or muscle bulges during joint motion [35]. It is less accurate than registration methods [36, 37]. In terms of routine clinical practice, it has been used only for the analysis of a patient's gait [12, 36]. It is a cumbersome method because of the need to attach reflective markers on the patient. On the other hand, the methods that use fluoroscopic videos and low-resolution MRI are applied primarily for medical research. They are not suitable for detailed joint diagnosis and surgery planning because the former exposes a subject to excessive radiation, whereas the latter is very costly.

3.3 Dynamic Musculoskeletal Models

Dynamic musculoskeletal models [14, 15, 16, 17, 18, 19, 20, 21, 22, 23, 24, 25, 26] model the poses of knee bones and forces over a range of flexion angles. In general, they include an abstract musculoskeletal model and a muscle model. The abstract musculoskeletal model includes abstract bones as well as abstract muscles and ligaments that are attached to the abstract bones (Fig. 7d). The abstract model can be calibrated in a similar manner as that in the kinematic model (Fig. 8). The muscle model is typically a **Hill-type model** [38] that describes a single muscle fiber or muscle element. The Hill-type model relates the force or tension on muscle and change of muscle length by a nonlinear equation. Zajac [39] modified the Hill-type model to model the force exerted by the tendon on the bone as a fraction of the maximum muscle force. In the simplest case, the fraction is known as the **muscle activation value**. In more elaborate cases, the fraction can also include cosine of the angle between the tendon and the muscle element, and the parameters for force-length and force-velocity relationships, which are represented as nonlinear curves. These parameter values, as well as the maximum muscle force, are estimated from biomechanical experiments on real muscle fibers [40]. During simulation, Hill-type model equations are used to compute muscle forces given muscle activation values, muscle lengths, and the model parameter values.

In addition to muscle forces acting on the bones, dynamic methods also compute **joint moments**. Although muscle generates linear force, joint motion is rotation about a rotation center. Therefore, joint moment is computed, which is the product of the force exerted by the muscle through tendon and the perpendicular distance of the force from the rotation center. For a joint with only rotational movement

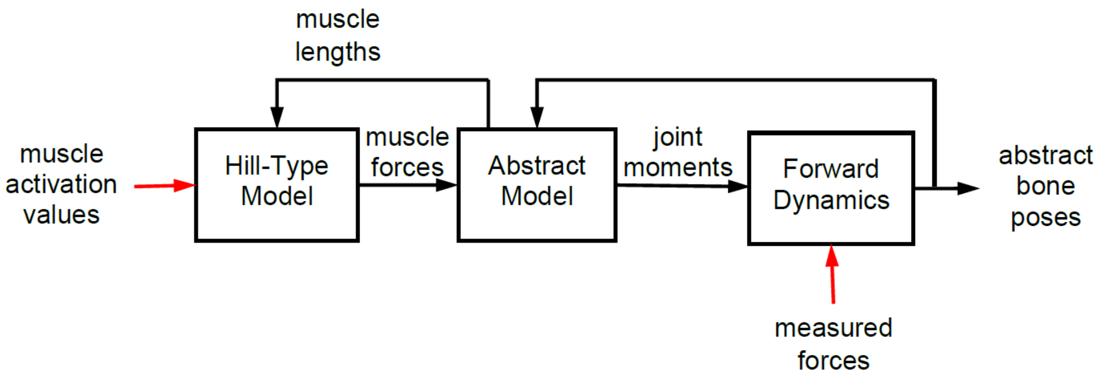

Figure 9: Generic dynamic method using forward dynamics. Red arrows: inputs, black arrows: outputs

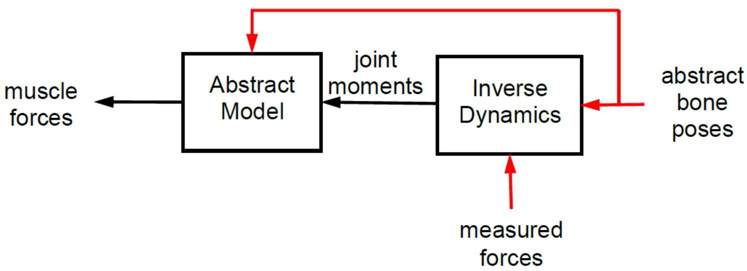

Figure 10: Generic dynamic method using inverse dynamics. Red arrows: inputs, black arrows: outputs

such as the shoulder joint, the rotation center is fixed. For a joint with rotational and translational movement such as the knee joint, the rotation center shifts as the knee flexes and extends.

A generic dynamic musculoskeletal system (Fig. 9) such as SIMM [14] and OpenSim [15, 16] requires the user to provide 3D geometric bone models, a joint model and muscle geometries (which is analogous to an abstract musculoskeletal model), joint kinematic data, and muscle model parameters for Hill-Zajac model. During knee motion generation or simulation, the user inputs muscle activation values. Then, the system computes muscle forces according to Hill-type muscle model, followed by joint moments according to muscle forces and the bone positions and joint angles. Next, **forward dynamics** [14, 15, 16, 20] is applied to compute abstract bone poses for the next time step according to the joint moments. The bone positions over time are then differentiated to obtain velocities and accelerations. Finally, 3D bone models can be aligned to the abstract bone poses in a similar manner as kinematic methods. Depending on the application, additional forces such as centripetal forces, coriolis forces, and gravitational forces can be included in the forward dynamic equation, which is balanced by measured ground forces acting on the subject's feet. Forward dynamic method is applied in [14, 15, 16] for analysing the functional consequences of surgery to patient's gait.

Another generic approach is to apply **inverse dynamics** [17, 18, 20] (Fig. 10).

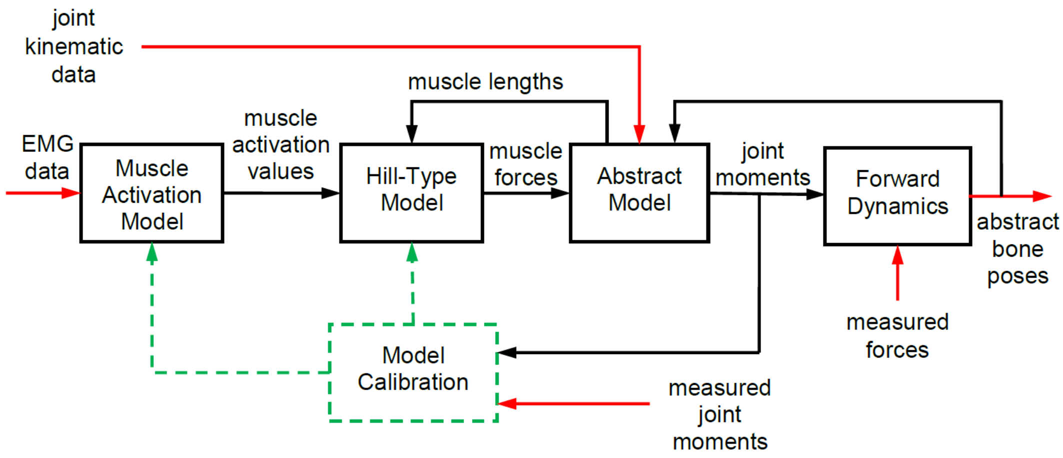

Figure 11: EMG-driven method. Red arrows: inputs, black arrows: outputs, green: model calibration.

Abstract bone poses over time are differentiated to obtain velocities and accelerations. Then, inverse dynamic method is applied on these joint kinematic data, and possibly measured forces, to compute joint moments. Then, muscle forces are computed from joint moments based on the abstract musculoskeletal model. The disadvantage of inverse dynamic method is that it is impossible to compute the muscle activation values from the muscles forces because the relationship between muscle activation value and muscle force is nonlinear and not invertible. Therefore, it is not appropriate for generating or simulating joint motion. Inverse dynamic method is applied in [17, 18, 20] for analysing the combination of muscle forces or joint moment from subject's gait.

In practice, it is difficult for the user to provide a sequence of muscle activation values over time for dynamic joint motion simulation. **EMG-driven method** [19, 20, 21, 22] (Fig. 11) mitigates this difficulty by introducing a **muscle activation model** that relates EMG signals and muscle activation values through nonlinear dynamic equations. EMG signals associated with joint motion are recorded in biomechanical experiments. In addition, mocap data can be recorded, along with EMG signals, for recovering joint kinematics, which are used to compute muscle lengths and velocities required by Hill-type model. EMG-driven method works as follows: First, EMG signal at a particular time step is used to compute muscle activation value according to the nonlinear dynamic equations in the muscle activation model. Next, muscle forces are computed from muscle activation values and muscle lengths and velocities according to Hill-type muscle model. Then, joint moments are computed from muscle forces and current joint positions and angles. After that, forward dynamics is applied to compute abstract bone poses at the next time step, and 3D bone models can be aligned to the abstract bone poses to produce 3D bone poses. For model calibration, the computed joint moments are compared with experimentally measured joint moments, and the difference between them are used to update the parameters of the Hill-type muscle model and muscle activation model. [20] proposes a variant of EMG-driven method that uses both forward and

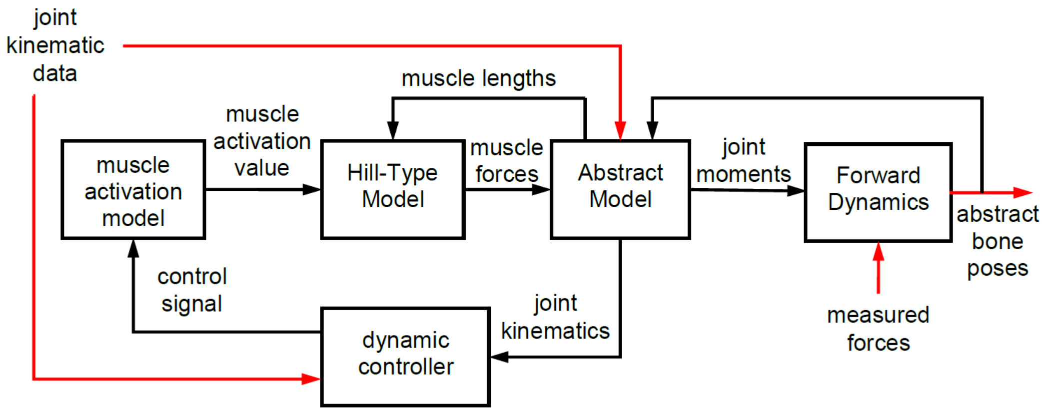

Figure 12: Computed Muscle Control method. Red arrows: inputs, black arrows: outputs.

inverse dynamics to overcome their weaknesses. EMG-driven method is used by [19, 20, 21, 22] for analysing gait and [23] for analyzing forces associated with wrist motion.

In practice, it is not possible to use EMG-driven method without EMG data that correspond to the required joint motion. **Computed Muscle Control (CMC)** method [24, 25, 26, 27] resolves this difficulty by providing a dynamic controller that produces control signals that are equivalent to EMG signals (Fig. 12). The dynamic controller compares the computed and measured joint kinematics to compute the control signal. The control signal is used by the muscle activation model to compute muscle activation values, which are then used to compute muscle forces, joint moments and abstract bone poses in the same manner as the generic forward dynamic method and EMG-driven method. Although the reference papers do not describe how to calibrate the model parameters of the muscle activation model and the Hill-type model, it is conceivable that these model parameters can be calibrated in the same manner as for EMG-driven method by comparing measured and computed joint moments. CMC method is used by [24, 25, 26, 27] for analysing forces associated with the gait.

Dynamic models can also estimate contact pressure of cartilages. In general, since the abstract bone models do not consider geometries of bones or cartilages, the bone or cartilage models may penetrate each other. The penetration distance and area between cartilages can be calculated using collision detection technique. Finally, they apply methods such as finite element [17, 21] or elastic foundation [18, 25, 26] to compute contact pressure based on cartilage material properties, penetration distances and area. Elastic foundation method is a linear method that is more efficient but less accurate than finite element method.

Dynamic models typically uses subject-specific 3D bone models and generic muscle models. So, the muscle model is not necessarily subject specific. Nevertheless, EMG-driven method and CMC method can include a calibration process that update the model parameters of Hill-type muscle model and muscle activation model. So, these methods can be subject specific. They model bone poses over a range of flexion angles. Moreover, they model forces such as muscle forces. Therefore, they can compute more information about knee joint mechanism such as contact pressure. For example, [17, 21] and [18, 25, 26] model PF and TF cartilage contact pressure, respectively.

Dynamic models are more complex than kinematic and static models because they also model forces. Methods for dynamic models require additional inputs and computation steps. Moreover, they have the same drawbacks as kinematic models since they use methods in kinematic models for model parameter estimation. Thus, these models have been used primarily for medical research only.

3.4 Summary

Comparisons of existing computational knee models are summarized in Table 1. All existing models can be subject specific. Among existing models, static models are the simplest and most accurate. However, they capture only a small number of poses and are, thus, unable to model knee joint motion. Kinematic models are more complex than static models. They incorporate both abstract models and 3D geometries of bones. Thus, they can model full range of knee joint motion. However, they are applied for analysing patient's gait only. Dynamic models are the most complex. They can model full range of knee joint motion and forces. However, they have been used primarily for medical research only.

In this research paper, a novel subject-specific model based on virtual cartilage is proposed for modeling PF joint motion (Section 4, 5). It is simple and easy to apply in routine clinical practice. It requires only one set of CT images to produce PF joint motion and it also models cartilages virtually. It is potentially more accurate than kinematic and dynamics models due to its fewer computations and thus fewer sources of errors.

4 Overall Research Problem

The overall goal of this research is to develop a subject-specific model of knee joint motion. To achieve this goal, the modeling process can be divided into three stages: (1) construction of subject-specific knee model, (2) estimation of knee bone poses, and (3) generation of knee motion. Construction of subject-specific knee model includes segmentation and construction of 3D geometries of knee bones at neutral pose from CT images. It can also include segmentation and construction of 3D geometries of soft tissues such as cartilages and menisci from MRI images. In addition, the attachment sites of tendons and ligaments can be obtained from MRI images. Estimation of knee poses over a range of flexion angles given the knee model is the most challenging part, and will be discussed in detail in the following paragraphs. After the knee poses are estimated, generation of knee motion can be easily achieved by replaying the estimated knee bone poses over the motion range.

Estimating knee poses is a complex and challenging task because it includes the articulation of both TF and PF joints. Incorrectly estimating the bone pose of one of the joints will affect the bone pose estimation of the other joint, thus producing incorrect overall knee pose. Moreover, bone pose estimation of each joint

Table 1: Comparisons of computational knee models.

(a) Overall comparison.

Model	**Subject specific**	**Knee motion**	**Simple**	**Clinical usage**
Static	Yes	No	Yes	No
Kinematic	Yes	Yes	No	Limited
Dynamic	Possible	Yes	No	No
Proposed	Yes	Yes	Yes	Yes

(b) Detailed comparison.

Model	**Model variant**	**# of CT/MRI**	**Other inputs**	**Soft tissues**
Static	—	> 1	No	Possible
Kinematic	3D-3D	$>= 1$	low-resolution MRI	Possible
	3D-2D	1	fluoroscopic video	Possible
	mocap	1	mocap data	Possible
Dynamic	generic	1	mocap data / joint kinematic data	Yes
	EMG-driven	1	joint kinematic data, EMG data, joint moments	Yes
	CMC	1	joint kinematic data, joint moments	Yes
Proposed	—	1	No	Virtual

is also influenced by the interaction between soft tissues. Therefore, the interaction between bones and soft tissues need to be modeled correctly for good estimation of knee poses. The general problem of estimating knee bone poses is defined as follows:

> Given a geometric knee joint model at neutral pose (0°), estimate the poses of the patella and tibia with respect to the femur over the full range of knee flexion angles.

As a start, this QE paper focuses on the PF joint, which is simpler than the TF joint due to the lack of menisci. For PF joint modeling, the first and third stages are similar to those discussed above. Figure 13 shows an example of PF bone models at neutral pose. The second stage is more involved. Without the tibia, the PF joint cannot directly model knee flexion angle, which is the angle between the femur and the tibia about the x-axis. Thus, the problem of estimating PF bone poses is defined as follows:

> Given a geometric PF joint model at neutral pose (0°), estimate the poses of the patella with respect to the femur over the full range of PF joint motion.

Details of the PF joint model and related algorithms are discussed in the next section.

5 Virtual Cartilage Model of PF Joint

The PF joint model consists of 3D geometries of the patella and femur (Fig. 13). Modeling of PF joint motion consists of three stages: (1) model construction (Section 5.1), (2) patella pose estimation (Section 5.2) and (3) patella motion generation (Section 5.3).

5.1 Construction of PF Joint Model

In the first stage, the 3D geometric bone models are directly constructed from a set of CT images of the knee at neutral pose. Next, at least three landmarks called **groove landmarks** (Fig. 14) are placed at distinctive features on the femoral groove. They are used to define a plane that is related to the motion of the patella with respect to the femur. Then, an additional landmark called **surface landmark** (Fig. 14) is placed around the medial area of femur surface. It is related to the lowest position of the patella with respect to the femur. The surface landmark is required since the TF joint is not modeled.

5.2 Estimation of Patella Poses

In 3D, the position and orientation of the patella with respect to the femur must be defined by at least three distinctive points on the patella. The sequence of positions of these three distinctive points traces out three motion paths. The main idea is to

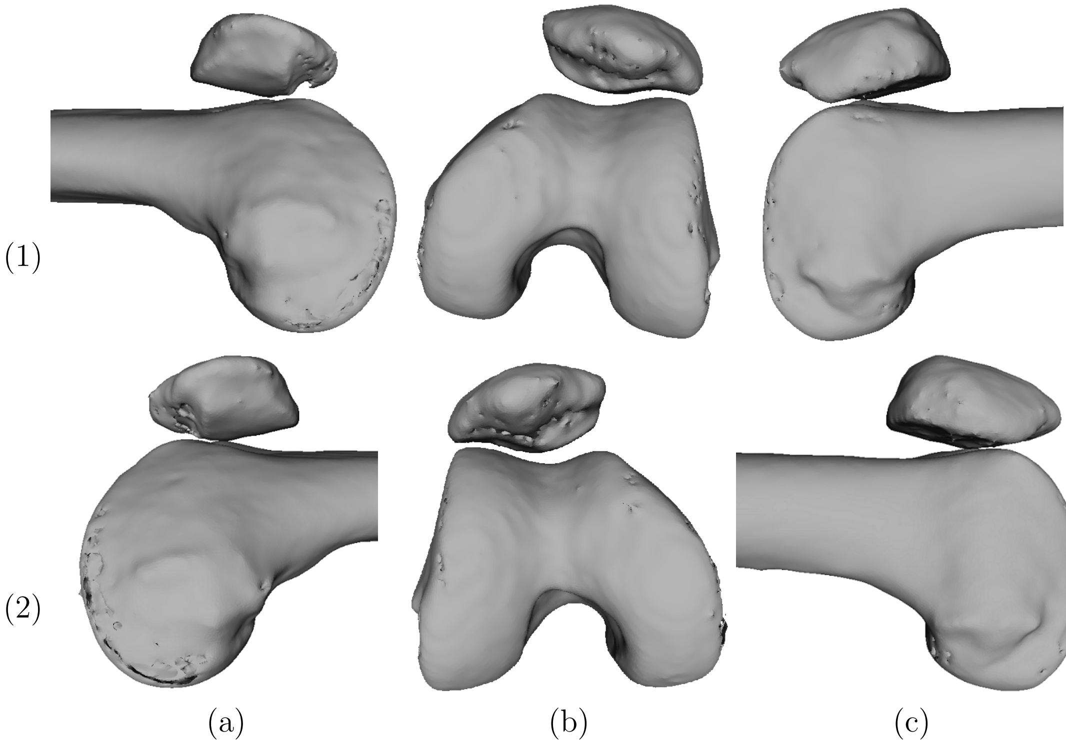

Figure 13: PF bone models of a real subject. (1) Left knee, (2) right knee. (a) medial view, (b) frontal view, (c) lateral view.

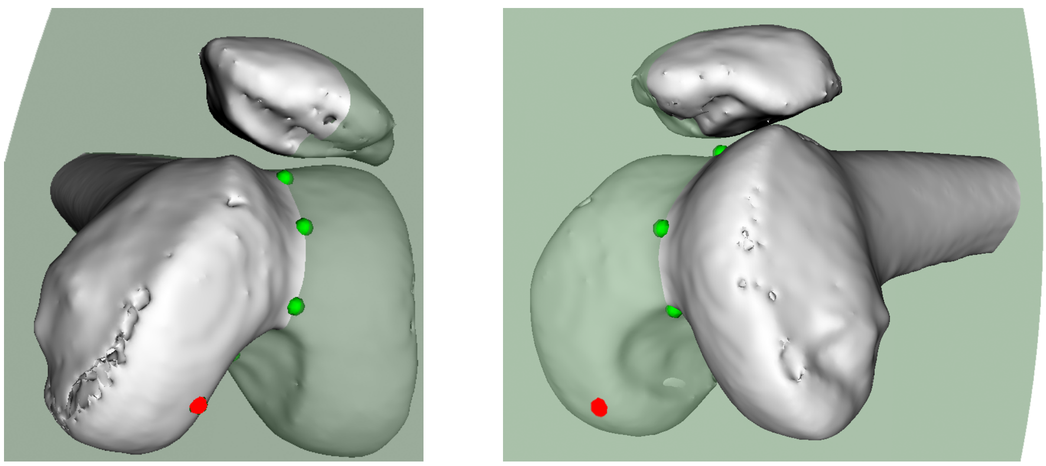

(a) (b)

Figure 14: Motion plane. Motion plane (green plane) is the plane that fits the groove landmarks (green dots). Surface landmark (red dot) is used to determine the end of patella motion.

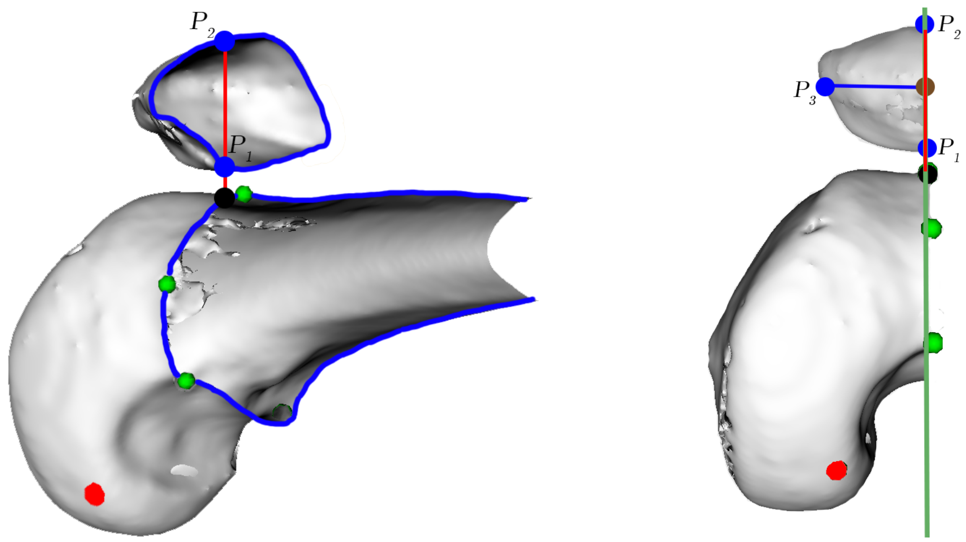

(a) (b)

Figure 15: Intersecting curves and distinctive points on the patella. Intersection curves (blue) are obtained by intersecting the motion plane (green) with the patella and femur models. One side of the patella and femur is removed for visual clarity. (a) Surface normal at the closets point on the femur (black dot) intersects the patella intersecting curves at two distinctive points P_1 and P_2. (b) Surface normal of motion plane (green line) at mid-point (brown dot) of the two distinctive points intersects the patella surface at a third distinctive point P_3.

determine these motion paths and then position the patella along the motion paths. The motion paths should describe correct motion of the patella.

To compute the motion paths, first a motion plane is constructed by fitting a plane to the groove landmarks (Fig. 14). The motion plane corresponds to the y-z plane and the normal of the plane is parallel to the x-axis. Therefore, the correctness of patella motion depends on the accuracy of the groove landmarks. The motion plane intersects the patella and femur models to generate intersection curves (Fig. 15a). As the subject's knee is captured at neutral position with the subject lying down, the patella is touching the femur. Thus, the distance between the closest points on the two intersection curves describes the combined cartilage thickness of the patella and the femur. The closest point on the femur relates to the starting point of the patella motion.

As described in Section 2, the patella will engage the groove of the femur as the knee flexes. Therefore, only the intersection curve on the groove of the femur is needed to define the patella's motion. To identify this part of the intersection curve, a plane that is normal to the motion plane and passes through the closest point on the femur and the last groove landmark is computed. Then, the intersection curve on the groove falls on the same side of the plane as the groove landmarks.

After identifying the relevant intersection curves, three distinctive points on the patella are identified (Fig. 15). First, the surface normal at the closest point on the femur intersects the patella intersection curve at two points, a closest point P_1

and a furthest point P_2 on the patella. These are two of the three distinctive points required. The distance between the closest points on the femur and patella is called the **closest distance** d_1, whereas the distance between closest point on the femur and the furthest point on the patella is called the **furthest distance** d_2. As the patella engages the femoral groove, it contacts two areas of the femur besides the groove (Fig. 6). Thus, the third distinctive point P_3 needs to be on one side of the patella. This point is obtained by intersecting the motion plane at the mid-point between the first two distinctive points and the one side of the patella (Fig. 15b).

Three motion paths are estimated for the three distinctive points on the patella (Fig. 16). The first motion path starts at the closest distinctive point P_1 and it is a curve that maintains a constant gap of d_1 from the intersection curve on the femoral groove. Similarly, the second motion path starts at the furthest distinctive point P_2 and it is a curve that maintains a constant gap of d_2 from the femur intersection curve. The third motion path is obtained by triangulating corresponding pairs of points on the first and second motion paths. Note that the first and second motion paths lie in the motion plane and the third motion path lies in a plane parallel to the motion plane. This ensures that the patella translates and rotates in the motion plane.

The three motion paths end near the last groove landmark (Fig. 16a). They are extended to model the full range of patella motion as follows. The extension of the third motion path starts at its ending point. Then, a plane parallel to the motion plane is fitted to the points in the third motion path. A new intersection curve on the femur which ends at a point in the new intersection curve that is closest to the surface landmark is obtained. Then, the same procedure as described above is used to obtain the extension of the third motion path from the intersection curve. Finally, the first two motion paths are extended by triangulation based on the extended third motion path. The three extended motion paths (Fig. 16b) describe a sequence of three positions for the three distinctive points of the patella over the full range of patella motion. As a result, the poses of the patella over its motion range is defined by the sequence of three distinctive points.

5.3 Patella Motion Generation

In motion generation stage, the sequence of patella poses over the full motion range is replayed (Fig. 17). Due to the lack of ground truth, quantitative verification of patella motion cannot be performed. Currently, verification is done by measuring the gap between patella and femur at each estimated patella pose. The computed gap is mapped to the femur surface with an appropriate color scheme for clarity of visualization (Fig. 17). The initial combined cartilage thickness measured at the knee's neutral pose is about 4 mm, which agrees with previous cadaveric study [41]. Gap size of about 2 mm to 4 mm corresponds to possible cartilage compression. Gap size less than 2 mm may correspond to modeling error if the femur and patella cartilages cannot compressed by more than 2 mm in total.

The virtual cartilage contact pattern is compared with the illustration of contact area in Figure 6 and results from previous work [42] (Fig. 18). In [42], the contact patterns are estimated and visualised in 3D based on manual observation from MRI

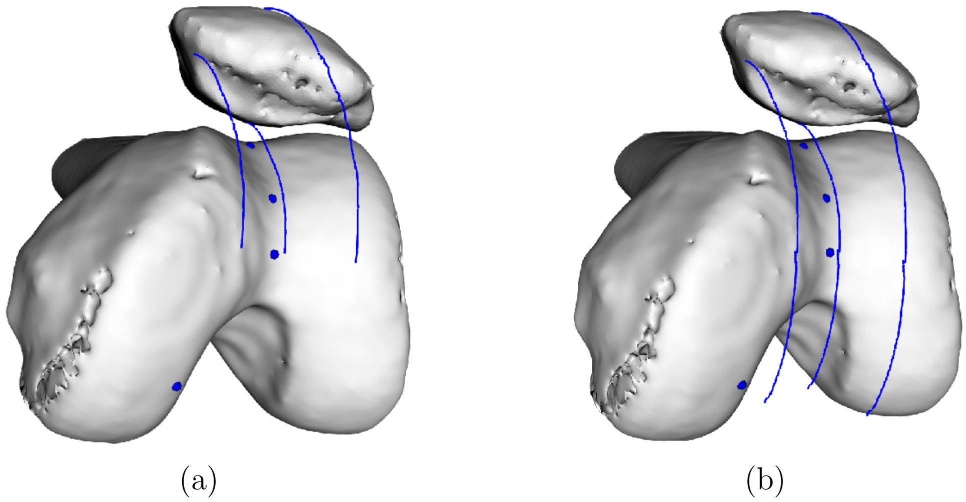

Figure 16: The three estimated motion paths. (a) Before motion paths extension and (b) after motion paths extension.

images of knee captured at 0° to 50° flexion angles in 10° increment. Similarly to Figure 6 and Figure 18, the contact area at the beginning of patella motion is smaller on the medial side and larger on the lateral side. Moreover, after the patella engages the groove the contact area is distributed onto both sides of the femoral groove.

6 Conclusions

This QE paper describes the initial research work of modeling PF joint. Existing models of knee joint motion include static models, which cannot model full range of knee motion, and kinematic and dynamic models, which are complex and used primarily for medical research only. In contrast, a novel model called virtual cartilage model of PF joint is proposed in this QE paper. Given the 3D geometries of the femur and patella and several landmarks, the virtual cartilage model generates motion paths that maintain their gaps from the femur. The motion paths lie on a motion plane which constraints the patella to translate and rotate in the motion plane. Qualitative comparison of contact area produced by the proposed model and previous work [42] shows similar contact pattern.

There are several gaps in the proposed method. First, the use of motion plane to estimate patella poses has not been validated quantitatively due to lack of ground truth. Secondly, without the ground truth, it is not possible to identify errors of the model for further improvement. Therefore, the next stage of this research is to work with our collaborating orthopedic surgeons in SGH to obtain ground truth data by scanning cadaveric knee at various flexion angles.

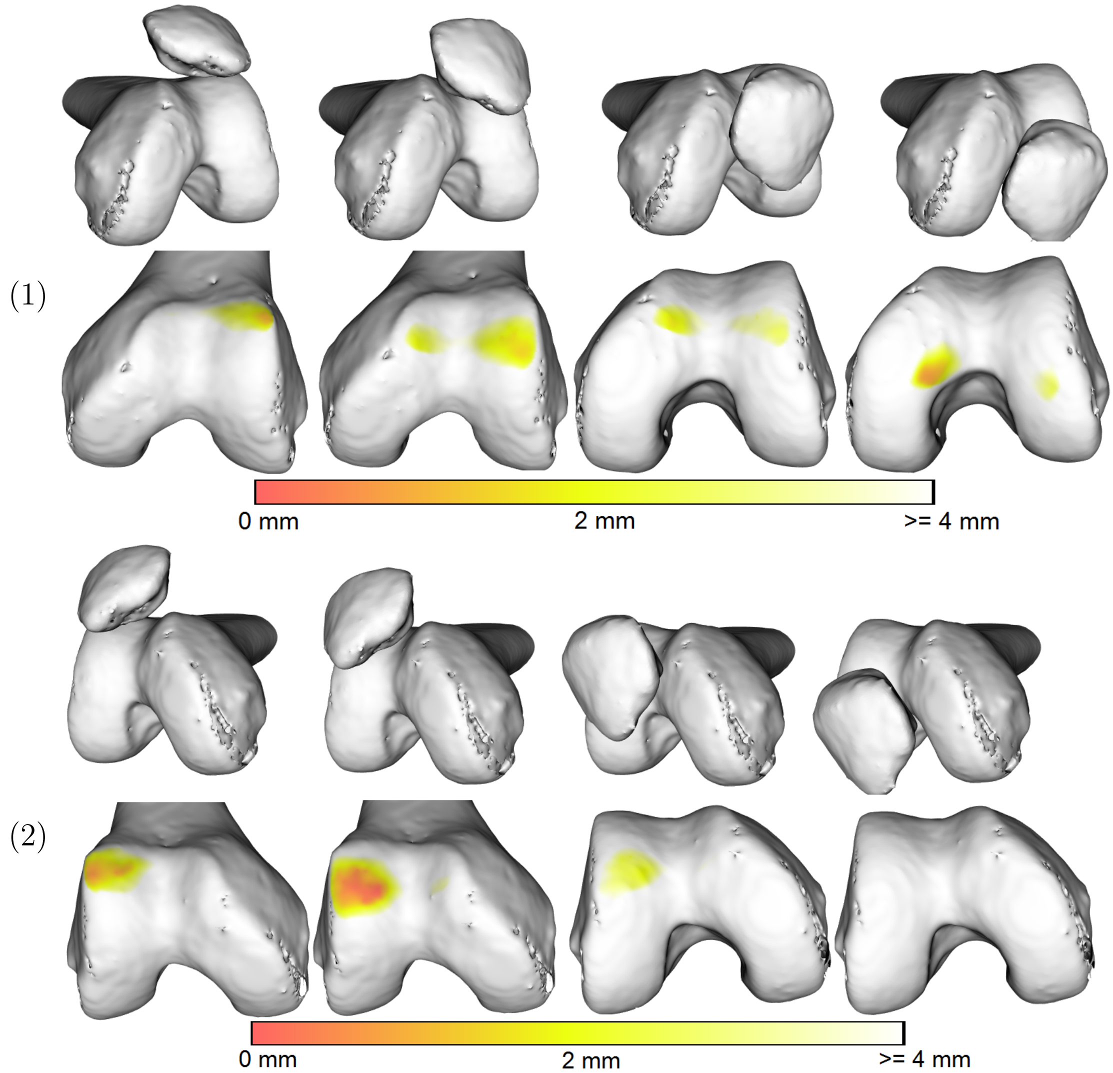

Figure 17: Patella motion generation and gap visualization. (1) Left knee, (2) right knee. Several estimated patella poses along the motion path (above) and their corresponding gap on the femur (bottom).

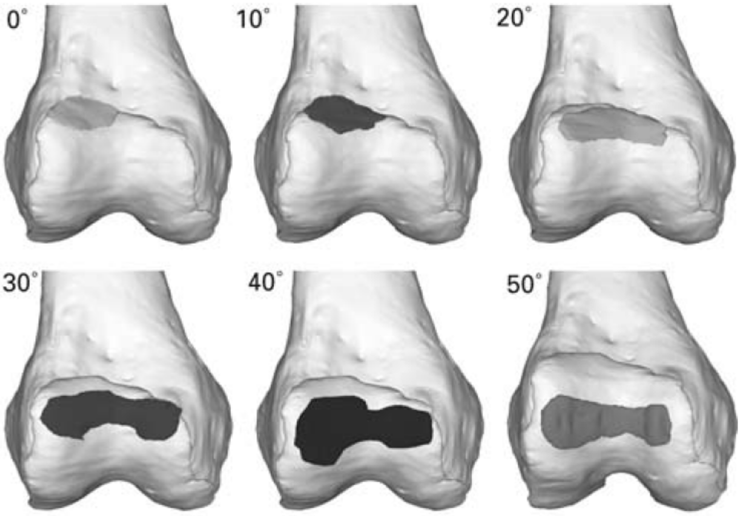

Figure 18: Contact area pattern used for qualitative comparison. Estimated patella contact on the femur for normal right knee [42].

Acknowledgement

This research is carried out in collaboration with Dr. Howe Tet Sen and his surgical team in Singapore General Hospital.

References

[1] R. Shenoy, P.S. Pastides, and D. Nathwani. Biomechanics of the knee and TKR. *Orthopaedics and Trauma*, 27(6):364–371, 2013.

[2] S.A. Oliveria, D.T. Felson, J.I. Reed, P.A. Cirillo, and A.M. Walker. Incidence of symptomatic hand, hip, and knee osteoarthritis among patients in a health maintenance organization. *Arthritis & Rheumatism*, 38(8):1134–1141, 1995.

[3] R.T.H. Cheung, N.W. Mok, P.Y.M. Chung, and G.Y.F. Ng. Non-invasive measurement of the patellofemoral movements during knee extension-flexion: A validation study. *Knee*, 20(3):213–217, 2013.

[4] M.A. Lafortune, P.R. Cavanagh, H.J. Sommer, and A. Kalenak. Three-Dimensional Kinematics of the Human Knee During Walking. *Journal of Biomechanics*, 25(4):347–357, 1992.

[5] S.Y. Song, C.-H. Pang, C.H. Kim, J. Kim, M.L. Choi, and Y.-J. Seo. Length Change Behavior of Virtual Medial Patellofemoral Ligament Fibers During In Vivo Knee Flexion. *The American Journal of Sports Medicine*, 43(5):1165–1171, 2015.

[6] Y.-S. Yoo, H.G. Chang, Y.-J. Seo, J.C. Byun, G.K. Lee, H. Im, and S.Y. Song. Changes in the length of the medial patellofemoral ligament: An in vivo analysis

using 3-dimensional computed tomography. *The American Journal of Sports Medicine*, 40(9):2142–2148, 2012.

[7] W.S. Jeong, Y.S. Yoo, D.Y. Kim, N.S. Shetty, P. Smolinski, K. Logishetty, and A. Ranawat. An analysis of the posterior cruciate ligament isometric position using an in vivo 3-dimensional computed tomography-based knee joint model. *Knee Surgery, Sports Traumatology, Arthroscopy*, 26(10):1333–1339, 2010.

[8] A.E. Kedgley, E.J. McWalter, and D.R. Wilson. The effect of coordinate system variation on in vivo patellofemoral kinematic measures. *Knee*, 22(2):88–94, 2015.

[9] R.A. Fellows, N.A. Hill, H.S. Gill, N.J. MacIntyre, M.M. Harrison, R.E. Ellis, and D.R. Wilson. Magnetic resonance imaging for in vivo assessment of three-dimensional patellar tracking. *Journal of Biomechanics*, 38(8):1643–1652, 2005.

[10] S. Hamai, N.J. Dunbar, T.A. Moro-Oka, H. Miura, Y. Iwamoto, and S.A. Banks. Physiological sagittal plane patellar kinematics during dynamic deep knee flexion. *International Orthopaedics*, 37(8):1477–1482, 2013.

[11] H.-C. Chen, C.-H. Wu, C.-K. Wang, C.-J. Lin, and Y.-N. Sun. A joint-constraint model-based system for reconstructing total knee motion. *IEEE Transactions on Biomedical Engineering*, 61(1):171–181, 2014.

[12] H. Kainz, L. Modenese, D.G. Lloyd, S. Maine, H.P.J. Walsh, and C.P. Carty. Joint kinematic calculation based on clinical direct kinematic versus inverse kinematic gait models. *Journal of Biomechanics*, 49(9):1658–1669, 2016.

[13] J.A. Reinbolt, J.F. Schutte, B.J. Fregly, B.I. Koh, R.T. Haftka, A.D. George, and K.H. Mitchell. Determination of patient-specific multi-joint kinematic models through two-level optimization. *Journal of Biomechanics*, 38(3):621–626, 2005.

[14] S.L. Delp and J.P. Loan. A computational framework for simulating and analyzing human and animal movement. *Computing in Science and Engineering*, 2(5):46–55, September 2000.

[15] S.L. Delp, F.C. Anderson, A.S. Arnold, P. Loan, A. Habib, C.T. John, E. Guendelman, and D.G. Thelen. Opensim: Open-source software to create and analyze dynamic simulations of movement. *IEEE Transactions on Biomedical Engineering*, 54(11):1940–1950, Nov 2007.

[16] A. Seth, M. Sherman, J.A. Reinbolt, and S.L. Delp. OpenSim: A musculoskeletal modeling and simulation framework for in silico investigations and exchange. *Procedia IUTAM*, 2:212–232, 2011.

[17] M. Akbarshahi, J.W. Fernandez, A.G. Schache, and M.G. Pandy. Subject-specific evaluation of patellofemoral joint biomechanics during functional activity. *Medical Engineering and Physics*, 36(9):1122–1133, 2014.

[18] Y.C. Lin, J.P. Walter, S.A. Banks, M.G. Pandy, and B.J. Fregly. Simultaneous prediction of muscle and contact forces in the knee during gait. *Journal of Biomechanics*, 43(5):945–952, 2010.

[19] D.G. Lloyd and T.F. Besier. An EMG-driven musculoskeletal model to estimate muscle forces and knee joint moments in vivo. *Journal of Biomechanics*, 36(6):765–776, 2003.

[20] T.S. Buchanan, D.G. Lloyd, K. Manal, and T.F. Besier. Estimation of muscle forces and joint moments using a forward-inverse dynamics model. *Medicine and Science in Sports and Exercise*, 37(11):1911–1916, 2005.

[21] T.F. Besier, G.E. Gold, G.S. Beaupre, and S.L. Delp. A modeling framework to estimate patellofemoral joint cartilage stress in vivo. *Medicine and Science in Sports and Exercise*, 37(11):1924–1930, 2005.

[22] P. Gerus, M. Sartori, T.F. Besier, B.J. Fregly, S.L. Delp, S.A. Banks, M.G. Pandy, D.D. D'Lima, and D.G. Lloyd. Subject-specific knee joint geometry improves predictions of medial tibiofemoral contact forces. *Journal of Biomechanics*, 46(16):2778–2786, 2013.

[23] D. Crouch and H. Huang. Simple EMG-Driven Musculoskeletal Model Enables Consistent Control Performance During Path Tracing Tasks. pages 1–4, 2016.

[24] D.G. Thelen and F.C. Anderson. Using computed muscle control to generate forward dynamic simulations of human walking from experimental data. *Journal of Biomechanics*, 39(6):1107–1115, 2006.

[25] D.G. Thelen, K. Won Choi, and A.M. Schmitz. Co-simulation of neuromuscular dynamics and knee mechanics during human walking. *Journal of biomechanical engineering*, 136(2):0210331–0210338, 2014.

[26] R.L. Lenhart, J. Kaiser, C.R. Smith, and D.G. Thelen. Prediction and Validation of Load-Dependent Behavior of the Tibiofemoral and Patellofemoral Joints During Movement. *Annals of Biomedical Engineering*, 43(11):2675–2685, 2015.

[27] OpenSim - Computed Muscle Control. `http://simtk-confluence.stanford.edu:8080/display/OpenSim/Computed+Muscle+Control`.

[28] J. Hamill, K. Knutzen, and T.R. Derrick. *Biomechanical basis of human movement*. Wolters Kluwer Health, 4th ed edition, 2015.

[29] BioDigital. `https://human.biodigital.com/`.

[30] D.B. Kettelkamp, R.J. Johnson, G.L. Smidt, E.Y.S. Chao, and M. Walker. An electrogoniometric study of knee motion in normal gait. *The Journal of Bone & Joint Surgery*, 52(4):775–790, 1970.

[31] T. Tischer, A. Geier, R. Lenz, C. Woernle, and R. Bader. Impact of the patella height on the strain pattern of the medial patellofemoral ligament after reconstruction: A computer model-based study. *Knee Surgery, Sports Traumatology, Arthroscopy*, 24(207):1–11, 2016.

[32] eOrthopod. `http://eorthopod.com/chondromalacia-patella/`.

[33] The Noyes Knee Insitute. `http://noyeskneeinstitute.com/unstable-kneecap/`.

[34] P.J. Besl and N.D. McKay. A method for registration of 3-d shapes. *IEEE Transactions on Pattern Analysis and Machine Intelligence*, 14(2):239–256, February 1992.

[35] A. Cappozzo, A. Cappello, U.D. Croce, and F. Pensalfini. Surface-marker cluster design criteria for 3-d bone movement reconstruction. *IEEE Transactions on Biomedical Engineering*, 44(12):1165–1174, Dec 1997.

[36] D.L. Benoit, D.K. Ramsey, M. Lamontagne, L. Xu, P. Wretenberg, and P. Renström. Effect of skin movement artifact on knee kinematics during gait and cutting motions measured in vivo. *Gait & Posture*, 24(2):152 – 164, 2006.

[37] M. Akbarshahi, A.G. Schache, J. W. Fernandez, R. Baker, S. Banks, and M.G. Pandy. Non-invasive assessment of soft-tissue artifact and its effect on knee joint kinematics during functional activity. *Journal of Biomechanics*, 43(7):1292 – 1301, 2010.

[38] A.V. Hill. The mechanics of active muscle. *Proceedings of the Royal Society of London B: Biological Sciences*, 141(902):104–117, 1953.

[39] F.E. Zajac. Muscle and tendon properties models scaling and application to biomechanics and motor. *Critical reviews in biomedical engineering*, 17(4):359–411, 1989.

[40] M. Blumel, S.L. Hooper, C. Guschlbauer, W.E. White, and A. Buschges. Determining all parameters necessary to build Hill-type muscle models from experiments on single muscles. *Biological Cybernetics*, 106(10):543–558, 2012.

[41] D.E.T Shepherd and B.B. Seedhom. Thickness of human articular cartilage in joints of the lower limb. *Annals of the Rheumatic Diseases*, 58(1):27–34, 1999.

[42] Y. Yamada, Y. Toritsuka, S. Horibe, K. Sugamoto, H. Yoshikawa, and K. Shino. In vivo movement analysis of the patella using a three-dimensional computer model. *Bone & Joint Journal*, 89-B(6):752–760, 2007.